JOURNAL OF GEOPHYSICAL RESEARCH, VOL. 103, NO. C8, PAGES 15,717-15,727, JULY 15, 1998

Short wave damping in the simultaneous presence of a surface film and turbulence

Jerome H. Milgram
Department of Ocean Engineering, Massachusetts Institute of Technology, Cambridge

Abstract. Spatial decay rates of short gravity waves and gravity-capillary waves in the frequency range of 3 to 8 Hz were measured in a laboratory wave tank equipped with a submerged oscillating grid to generate turbulence. Experiments were conducted with: clean fresh water, fresh water with an oleyl alcohol insoluble surfactant surface film, fresh water with a Triton X-100 soluble surfactant surface film, and with sea water having a surface film of its own natural surfactants. With each material, decay rate tests were conducted with and without turbulence. The principal purpose of the study was to determine the extent to which turbulence modified the wave decay due to the presence of surface films. This is of importance for modeling the energy balance of short sea waves which influence microwave backscattering used for remote sensing of the ocean. The results show that the wave decay rate is equal to the sum of the rates due to surfactant alone and with turbulence alone. It is concluded that the statistically stationary component of the turbulence that exists near the free surface does not significantly modify the decay mechanism associated with the presence of the surfactant.

1. Introduction

The energy balance of short sea waves, which play an important role in microwave backscattering from the ocean surface, includes wind energy input, nonlinear wave-wave interactions, modulation by currents, interactions with turbulence and damping due to surface films [*cf. Snyder et al.*; 1981; *Milgram et al.* 1993]. The aim here is to gain an understanding of the combined influence of turbulence and surface films. In particular, it is of interest to determine if the wave decay is the sum of the surfactant and turbulence effects individually or whether the turbulence augments the damping due to surface films by increasing the mixing of momentum in the oscillating free surface boundary layer where most of the film-induced wave energy dissipation occurs.

The fundamental theory for the decay of short waves by surface films, often called "the Marangoni wave damping theory" (MWDT) or the Marangoni effect (other phenomena are also called the "Marangoni effect") is well established in the developments presented by *Dorrestein* [1951], *Lucassen-Reynders and Lucasssen* [1969] , *Hansen and Ahmad* [1971], *Lazarev and Pokazeyev* [1986], *Cini et al.* [1987], *Alpers and Huhnerfuss* [1989] and many others. The surface film elasticity E plays a dominant role. Some researchers have advanced the hypothesis that the surface viscosity of the film, μ_s, and frequency dependence of E play a significant role in wave decay. The experiments of *Mass and Milgram*, this issue, (hereinafter referred to as M&M), agreed with others in confirming the MWDT. However, M&M found that the parameters to be used in the MWDT that resulted in the best agreement with experiments were the frequency-independent quasi-static value of E and zero surface viscosity, for oleyl alcohol and natural seawater surfactant films for the 0 to 25 Hz frequency range of their experiments. Obviously, there must be some small surface viscosity, but M&M found that this was too small to influence the wave decay and certainly less than 0.05 mN s/m for the films they studied.

The mechanisms of wave decay and the depth scales over which they take place are of importance. In the case of wave decay due to an elastic or viscoelastic film, the tangential gradient of the surface tension, which is made nonuniform by the wave-induced surface distortions, must be balanced by the tangential components of the shear stress in the bulk fluid just beneath the film. From the derivation of the flow quantities given by *Hansen and Ahmad*, [1971] the depth of the surface-induced laminar boundary layer is approximately $\sqrt{\nu T}$. At this depth the boundary layer motion is diminished by about 90% from its surface value. ν is the kinematic viscosity of the bulk water and T is the wave period. This depth is very small. As an example, for 3 Hz waves it is 0.6 mm. The viscous dissipation of wave energy in this thin layer is responsible for most of the damping of waves due to surface films.

Paper number 98JC01191.
0148-0227/98/98JC-01191$09.00

The mechanism by which turbulence in clean water causes wave decay was put forth by *Boyev* [1971], and the effect was shown in experiments by *Green et al.* [1972] and *Skoda* [1972]. *Kitaigorodskii and Lumley* [1983] put the mechanism on a firmer theoretical footing by deriving its governing equations from first principles. *Olmez and Milgram* [1992] (hereinafter referred to as O&M) conducted an experimental study to quantify the wave decay due to turbulence in terms of wave and turbulence parameters. These investigations led to the conclusion that the mechanism of wave decay by turbulence is downward turbulent convection of wave kinetic energy out of the wave energy-containing region which is about $\lambda/4$ (λ is the wavelength) thick. Approximately 95% of the kinetic energy lies above this depth. For 3 Hz waves this energy-containing region is about 44 mm thick. Thus for typical short waves, the depth involved in turbulence-induced wave energy loss is much greater than the depth involved with surface film-induced wave energy loss.

The essential issue that is addressed here is whether the presence of turbulence has a significant influence on the short wave decay rate caused by the presence of a surface film. In particular, the question that naturally arises is whether or not the turbulent mixing in the thin free surface boundary layer augments the wave energy dissipation in this layer. In order to answer this question, experiments were conducted in which decay rates were measured in the presence of a surface film, with and without the presence of turbulence, and compared with theoretical predictions for the individual contributions to the rates.

2. Apparatus and Measurement Methods

2.1. Tank With Wave and Turbulence Generators

The experiments were conducted in a tank with horizontal dimensions of 3.65 m x 3.65 m and filled with water to a depth of 0.76 m. A plunger type wave maker with a wedge-shaped cross section runs the entire width of the tank along one edge and an 8° sloping beach runs along the entire 3.65 m width of the opposite edge. The length of the beach along its slope is 40.6 cm.

It is necessary to be able to skim surface films off the water before adding known surfactants to fresh water. For these experiments, the tank was filled with tap water which was left stationary for about 1 day during which most of the small quantity of surfactant in it accumulated on the surface which was then skimmed. The beach was temporarily raised to expose an overflow weir located a few centimeters from the tank wall, running the full width and sealed to the tank walls, which was be operated as a surface skimmer. The space behind the weir was connected to drains whose valves were open to skim the surface and closed to conduct wave tests. Skimming was aided by air bubble plumes coming from three perforated copper pipes running on the tank bottom along its full width and parallel to the skimmer. The first of these is at the bottom corner immediately under the wave maker. The second is 1.25 m closer to the weir and the third is another 1.25 m closer still. During skimming, water was very slowly added to the tank so a slow waterfall forms over the entire length of the weir. Initially, air was supplied to the perforated pipe under the wave maker. The rising bubble plume entrains water which turns horizontally toward the weir at the surface, and this flow carries surface material along with it. When the surface between the first and second perforated pipes was clean, air was supplied to the second pipe. Its bubble plume turns horizontally at the surface with one portion moving towards the weir and one towards the wave maker. Since air was still supplied to the pipe beneath the wave maker, there was little, if any, recontamination of the surface between the two pipes. Then, when the surface was clean up to the third pipe, its air supply was turned on and the remaining surface material was driven over the weir. Surface cleaning would occur with just the water addition and the resulting waterfall over the weir, but the bubble plume induced flow makes it happen much faster.

Turbulence was generated with a vertically oscillating submerged grid whose upper surface has a mean position 0.33 m above the tank bottom. The grid is made of 2.7 cm square bars on 11.6 cm centers running both along and across the tank from wall to wall. It has two rollers mounted on its lower surface along each edge at the quarter-length positions to maintain a gap of a few millimeters at each tank wall. A mechanism beneath the grid and driven through shafts that go through seals in the tank walls near the bottom by an electric motor outside the tank oscillates the grid with a sinusoidal vertical motion. For the experiments reported here, the grid stroke (double-amplitude) was 15 cm and the grid oscillation frequency was 0.9 Hz.

2.2. Surface Tension and Elasticity Measurement

To determine elasticity E versus surface tension T, samples of the surface material and the underlying bulk fluid were transferred with a beaker from the large test tank to the longitudinal trough described in M&M. This trough has dimensions of 80 cm long x 16.5 cm wide x 2.5 cm deep. It has paraffin-coated anodized aluminum surfaces and in use was filled to the extent that the fluid surface bulged above the upper plane of the trough. Surface tensions were measured with a Wilhelmy plate hung from an electronic balance as described in M&M. The surface film was compressed and expanded by moving a paraffin coated Lucite bar that was across the trough and in contact with both the fluid surface and the top longitudinal surfaces of the trough. The elasticity is defined in the usual way as

$$E = \frac{dT}{d\ln(\mathcal{A})} \quad (1)$$

Both E and T depend on $\mathcal{A}$ in the elasticity determination experiment, and the function of E versus T was determined for each surfactant tested. Except where noted otherwise in section 7, surface tension versus area was measured the same way as by M&M. This was to move the surface-touching bar to change the area by about 5% during a time of about 5 s, wait about 15 s for the surface tension to become constant, measure it by means of the force on the Wilhelmy plate with computer-interfaced data, and repeat the process until the whole area range was included.

When wave decay experiments were conducted in the large tank, the surface tension was measured before the waves were started at each test frequency, again using a Wilhelmy plate suspended from an electronic balance. For these experiments, the balance was supported by a bridge over the water surface which was supported by two opposite tank walls.

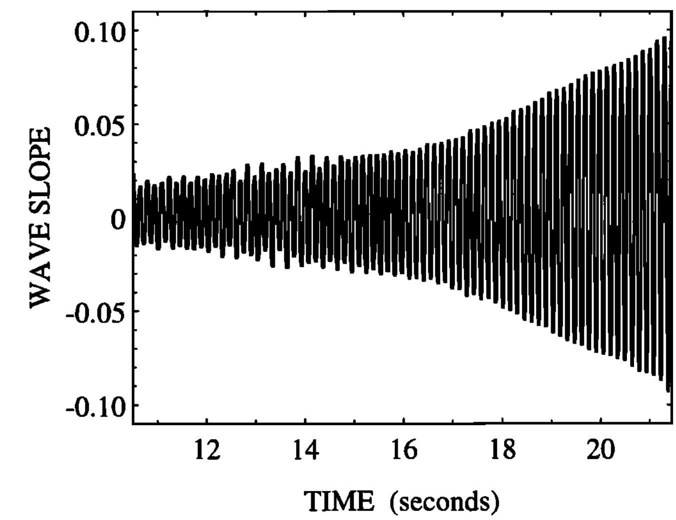

Figure 2. Wave slope versus time measured with a towed laser slope gauge. These data are for 5.85 Hz waves on a seawater surface having an adsorbed surfactant film.

2.3. Measurement of Wave Slope Versus Position

The apparatus for measuring wave slopes is sketched in Figure 1. Four laser slope gauges were affixed to a carriage that rode on a beam spanning the tank in the direction of wave propagation. These were the same gauges that were used and described by M&M in which the deflection of a laser beam reflected from the surface is detected by a SiTek Model IL-30SP semiconductor position detector with position converted to a ± 10 V signal by an On-Trak Photonics Model OT-300 signal conditioner. The resulting slope signal was digitized by an analog-to-digital converter at a rate of 200 Hz per channel and recorded in a digital computer file.

The wave gauge carriage was towed with a 3 mm diameter rope at a speed of 5 cm/s by a pulley driven by an electric motor having a digital encoder on its shaft. The encoder output, which provided carriage position versus time, was sampled at a rate of 200 Hz, and the samples were stored in the same file as the measured wave data. Traction between the pulley and the rope was achieved by wrapping the rope $1\frac{1}{4}$ turns around the pulley and hanging a weight on the end of the rope. The carriage was towed toward the wave maker when acquiring experimental data. Between data runs, the carriage was moved manually to its start position.

Four wave slope gauges at differing longitudinal and transverse positions were used so the wave decay rates measured by each of them could be averaged together. Because the tank width is so much larger than the wavelengths used, wave maker corner effects on the measurements were negligible, and all four wave gauges mea-

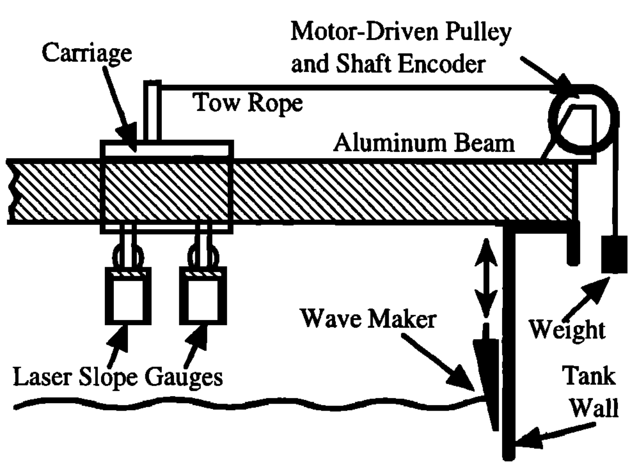

Figure 1. Apparatus for measurement of wave slope versus position. Two for the four slope gauges are shown for clarity. The gauges are laterally displaced (into the page) from each other.

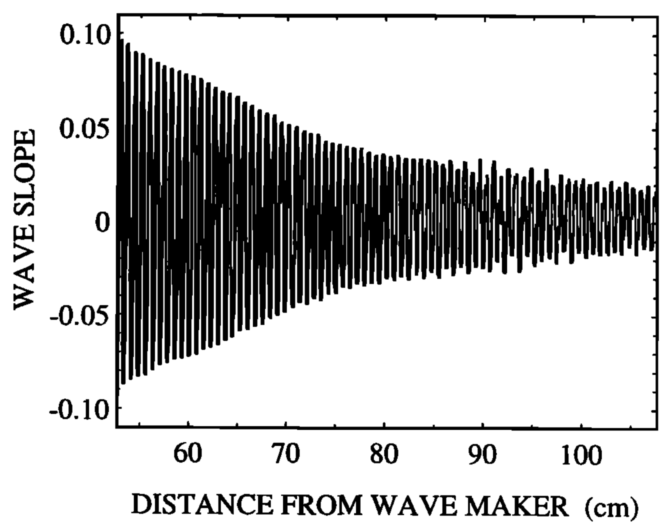

Figure 3. Wave slope versus position measured with a towed laser slope gauge.
This is for the same waves shown in the Figure 2.

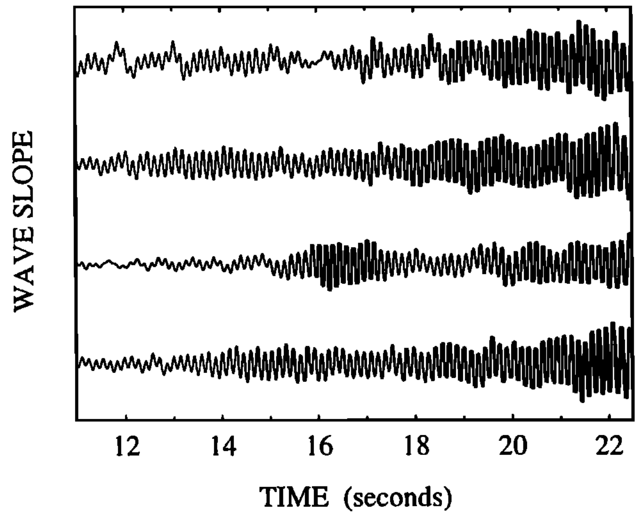

Figure 4. Wave slope versus time simultaneously measured with four towed laser slope gauges in different locations in the presence of turbulence. These data are for 5.85 Hz waves on a seawater surface having an adsorbed surfactant film and were acquired immediately after the data without turbulence used for the two Figures 2 and 3.

sured nearly the same decay rates in the absence of turbulence. Figure 2 shows a typical result for measured wave slope versus time from the moving carriage in the absence of turbulence. The amplitude of the slope signal increased with time because the carriage was towed towards the wave maker. The corresponding slope versus position signal is shown in Figure 3.

In the presence of turbulence, however, the local wave amplitude does not vary smoothly with position because the turbulence randomly scatters the waves in all directions in addition to attenuating them. Figure 4 shows the waves slopes versus time measured by all four wave gauges for the same wave maker conditions leading to Figures 2 and 3, but in this case, turbulence is present. In these irregular conditions, averaging the decay rates from four instruments in different locations leads to results having less variance than those from a single wave gauge.

2.4. Surface Elevation Measurement

Experiments with a clean water surface were conducted before the laser slope gauges and the gauge towing system were built. For the clean surface experiments, wave elevations were measured with four resistance wire wave gauges. In each gauge the resistance between two 30-gauge nichrome wires spaced 3 mm apart was measured as a function of time. These gauges were stationary and spaced 29 cm apart in the direction of wave propagation. Data acquired with these gauges were sampled at 128 Hz per gauge and digitized and stored in computer disk files. The period of each data run was 64 s so there were 8192 data points per channel. This fairly lengthy data acquisition period was used to reduce the variance in measured wave amplitudes caused by the turbulence. The spatial decay rates were based on the amplitudes measured at the four gauge locations.

On occasion, the amplitude time history from one of the gauges would be very different from the others, largely due to the effects of turbulence in its vicinity. In these instances, the decay rates from the remaining three gauges were averaged together to obtain a representative decay rate.

2.5. Turbulence Measurement

Horizontal and vertical components of turbulence velocities were measured with hot film anemometers composed of a Dantec Model 55R61 two component fiber-film X-probe and two Dantec Model 56C anemometers. The probe was mounted on a rotating arm driven by an electric motor such that the probe traversed a 0.65 m radius horizontal arc with a swept angle of 200°. The probe support can be moved vertically in its mount on the rotating arm in order to obtain turbulence data over a range of heights. Calibration data were obtained by operating the rotating arm over a range of speeds. Although the anemometer system had built-in linearizers, more accurate fluid velocities were obtained on the basis of the calibration data in the computer program which analyzed the data.

3. Surfactants Used in the Experiments

Experiments were conducted in clean water with a clean surface and with three different surfactants. The clean water experiments were done to confirm the validity of the empirical relation for wave decay by turbulence determined by O&M, for the apparatus and conditions of the surfactant experiments. The empirical relation was based on data obtained with axisymmetric waves, whereas the surfactant experiments used two-dimensional waves, and the turbulence generator was slightly different. Whereas the turbulence grid occupied the entire horizontal plane of the tank in the surfactant experiments, a similar grid, but with higher solidity, occupied only a portion of a much larger tank in the O&M experiments. That grid caused bulk vertical fluid motion at the grid frequency above it and this generated a significant wave field at the grid oscillation frequency which coexisted with the separately generated waves whose decay rate was being measured. The bulk fluid motion cannot occur when the grid occupies the entire horizontal plane due to the constant volume of fluid surrounding the grid, so for the surfactant experiments the component of wave elevation at the grid oscillation frequency was much smaller.

The basis of development for the empirical relation between turbulence and wave decay is such that it should be independent of the presence of a wave field at the grid frequency, but that needed to be confirmed here. Experiments at only a few frequencies were conducted with a clean surface since they confirmed the empirical relation for decay due to turbulence (section 6.2).

Experiments were conducted at more frequencies for each of the surfactants studied. The surfactant films used were oleyl alcohol [*Z*-9-octadecen-1-ol, $CH_3(CH_2)_7CH{:}CH(CH_2)_8OH$] on clean fresh water, to obtain results for an insoluble pure substance film, Triton X-100, which is a polyethylene oxide with a molecular weight of 628 purchased from Sigma-Aldrich Corporation, mixed with clean fresh water at a concentration of 0.5 x 10^{-6} molar, to obtain results for a pure substance soluble surfactant, and an adsorbed natural surfactant film from seawater, to obtain results representative of wave decay effects in the ocean. The seawater was taken from the harbor at Hampton, New Hampshire, during an incoming tide and in a current to obtain water that had recently been in the ocean. It was carried from the harbor to the laboratory in a tank truck that had recently been flushed several times to minimize the possibility of contamination by other surfactants. Also, the water was pumped from a small distance above the bottom of the truck tank to the laboratory tank without the truck being completely emptied to avoid pumping any material from the water surface in the truck. Any particulate matter of visible size in the water was trapped in a filter at the tank truck hose outlet in the laboratory.

The surfactant film that adsorbed onto the surface of the water in the laboratory tank could not have exactly the same mixture of organic surfactants that existed on the surface in the harbor. Rather it was chosen as a film made of natural oceanic surfactants that could be achieved in the laboratory.

4. Turbulence Analysis and Description

Turbulence was measured at depths between 0.3 and 5.0 cm and in the absence of waves since they would cause a varying depth at the hot film probe during a measurement. The anemometer voltage signals were digitized at a rate of 200 Hz per channel by a computer-interfaced analog-to-digital converter and stored as computer files which were then processed by analysis computer programs. The digitized voltages were converted to vertical and horizontal velocities, point-by-point, using the previously obtained calibration data for the anemometers. These velocity data were then processed into two wavenumber spectra following the procedure O&M used for the single velocity component they measured. The "frozen turbulence" approximation was used to transform frequency (f_τ) spectra into horizontal wavenumber (k_τ) spectra. This relates wavenumbers to frequencies on the basis of the probe speed, U_p, by

$$k_\tau = \frac{2\pi}{U_p} f_\tau \qquad (2)$$

Turbulence spectra were based on averages from three data acquisition runs of time period t_p =20.48 s (4096 data points) each. The horizontal and vertical velocities for each of these runs are called $u_{1j}(t)$ and $u_{2j}(t)$,respectively, where $j = 1,2,3$, and the Fourier transforms of these functions, obtained computationally with a fast Fourier transform (FFT) algorithm, are called $U_{1j}(f_\tau)$ and $U_{2j}(f_\tau)$. Raw, one-sided, frequency power spectra were computed as

$$S_m^{(r)}(f_\tau) = \frac{2}{3t_p} \sum_{j=1}^{3} |U_{mj}(f_\tau)|^2 \qquad (3)$$

The multiplication by 2 is to make the spectrum one-sided. $m = 1$ corresponds to the horizontal velocity spectrum and $m = 2$ corresponds to the vertical velocity spectrum. Smoothed frequency spectra, $S_m^{(s)}(f_\tau)$, $m = 1,2$, were then obtained by convolving the raw spectra with a Parzan spectral window (cf. *Jenkins and Watts*, 1968, Chapter 6) having a corresponding autocorrelation window length of $\frac{t_p}{4}$:

$$S_m^{(s)}(f_\tau) = S_m^{(r)}(f_\tau) \otimes \frac{3}{16} t_p \left[\frac{\sin(\pi f_\tau t_p/8)}{\pi f_\tau t_p/8}\right]^4 \qquad (4)$$

The spectra were truncated at $f_{\max}$ = 20 Hz, which corresponds to $k_{\max}$ = 10.74 rad/cm, at which the spectral levels were less than 0.5% of their low-frequency values.

Finally, the wavenumber spectra were calculated from the frequency spectra according to

$$S_m(k_\tau) = \frac{U_p}{2\pi} \left| S_m^{(s)}(f_\tau) \right|_{f=k_\tau U_p/2\pi} \qquad (5)$$

As an example, Figure 5 shows the horizontal and vertical velocity wavenumber spectra at a depth of 2 cm beneath a clean water surface. Figure 5 contains a line with slope corresponding to $k_\tau^{-5/3}$ to demonstrate the inertial subrange. The vertical position of this line

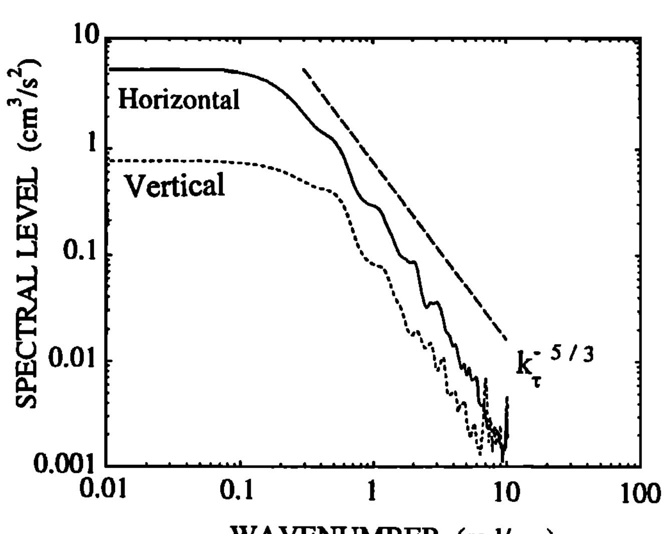

Figure 5. Turbulence spectra at a depth of 2.0 cm.

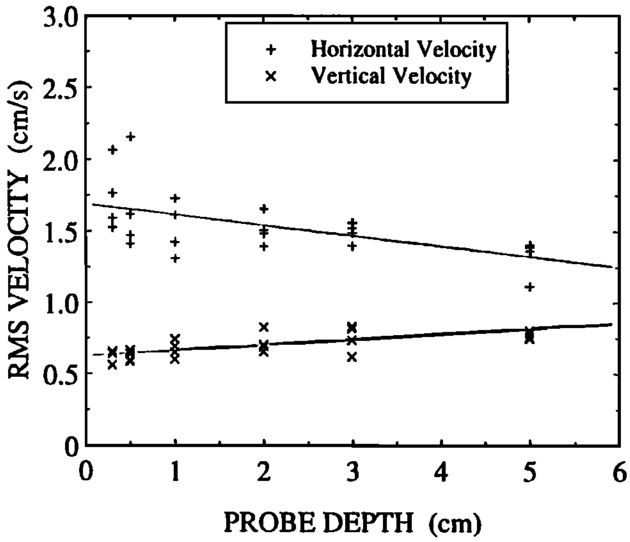

Figure 6. Horizontal and vertical turbulence velocities. Lines in this and Figure 7 are straight line fits to the data.

is arbitrary and was chosen for Figure 5 on the basis of visibility.

The horizontal and vertical rms turbulence velocities, u'_1 and u'_2, and integral length scales, L_1 and L_2, were determined from

$$u'_m = \left[\int_0^{k_{max}} S_m(k_r) dk_r \right]^{1/2} \tag{6}$$

$$L_m = \frac{\pi}{2} \frac{S_m(0)}{(u'_m)^2} \tag{7}$$

Figures 6 and 7 show the rms velocities and the length scales, respectively, for the range of experimental probe depths for several sets of measurements. No significant difference was found between the results with a clean water surface and a surface with an oleyl alcohol film. This is consistent with the presumption that the surfactant influences the grid-generated flow principally in a surface viscous sublayer whose thickness L_v is estimated as

$$L_v \approx \sqrt{\frac{\nu L_1}{u_1}}. \tag{8}$$

Turbulence measurements were made at depths of 3 mm and more because the free surface was observed to influence the flow at the probe for shallower depths. For the grid-generated turbulence in this study this estimate of L_v from equation (8) is 1.6 mm which indicates the turbulence measurements were below the viscous sublayer. Only a single turbulence condition was used in the experiments because its influence on wave decay was substantially less than the influence of the surfactant films while being the most intense turbulence the apparatus could generate reliably.

5. Wave Analysis Procedures

In the absence of turbulence the measured wave amplitudes have nearly an exponential dependence on propagation distance and are constant at a fixed location. However, in the presence of turbulence there is a time dependence of the amplitude due to wave scattering by the turbulence as well. The approach taken in estimating wave amplitude is based on the wave energy in a modest frequency range surrounding the fundamental wave frequency and excluding the effects of energy at distant frequencies. This captures most of the scattered, but still existing, wave energy and includes it in the analysis. It also captures the wave energy in the presence of the spectral spreading that results from the varying amplitude associated with the motion of the laser slope gauges.

The first step was to calculate a raw one-sided power frequency spectrum, $S_w(f)$, from the wave data at a specified location as

$$S_w(f) = \frac{2}{t_r} \left| \int_{t_s}^{t_s+t_r} \zeta(t) e^{-i2\pi f t} dt \right|^2 \tag{9}$$

where t_r is the time record length under consideration, t_s is the time at the start of the record, and ζ is the measured quantity which was surface elevation or surface slope depending on which gauges were in use. For measurements with the fixed location surface elevation gauges, t_r = 64 s. Equation (9) was computed with an FFT algorithm.

With the moving laser slope gauges, a value of t_r = 2.56 s was used. The centers of successive records were spaced 1.28 s apart (corresponding to a gauge movement of 6.4 cm) and as a result the data records overlapped by half the record length.

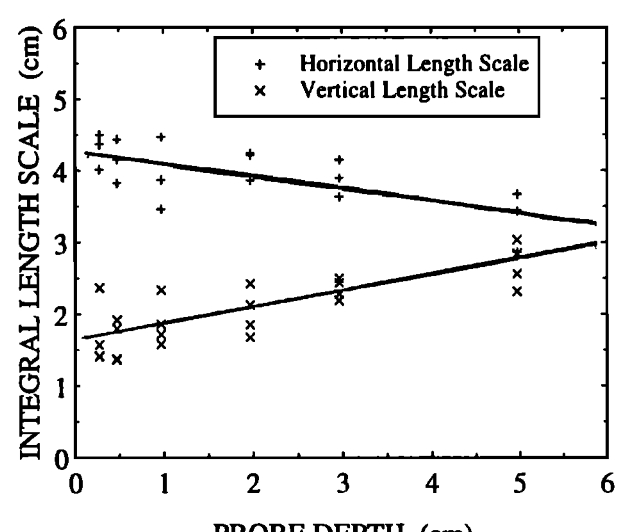

Figure 7. Horizontal and vertical integral length scales.

Then, for the location under consideration the wave amplitude, a, was estimated as

$$a = \left[2 \int_{f_j-\Delta f}^{f_j+\Delta f} S_w(f) df \right]^{\frac{1}{2}} \quad (10)$$

where f_j is the frequency for which $S_w(f)$ is maximum and $2\Delta f$ is the width of the frequency band upon which the amplitude is based. With the wave elevation data, Δf was chosen to be 0.75 Hz which resulted in 96 Fourier coefficients being included in the sum for the discrete form of (10).

With the wave slope data, Δf was chosen as 1.76 Hz which resulted in nine Fourier coefficients included in the sum for the discrete form of (10). In this case, the value of Δf is a compromise between it being a modest fraction of the wave frequency and the data variance reduction associated with inclusion of more Fourier coefficients. The difference between the choices for the fixed and moving gauges occurs because of the disparate record lengths of 64 s and 2.56 s.

The wave amplitude a versus propagation distance x takes the following form for both surface film and turbulence induced wave decay, and it is used as the basis for decay when both influences exist simultaneously as well:

$$a(x) = a_o e^{-\alpha x} \quad (11)$$

which is equivalent to

$$\ln a(x) = \ln a_o - \alpha x \quad (12)$$

For each set of measurements of amplitude versus propagation distance, the decay rate α was taken as the negative of the slope of the straight line fit to the $\ln a(x)$ versus x data having minimum mean squared error.

6. Bases for Comparison With Experimental Data

The principal goal of this study is to compare measured decay rates in the simultaneous presence of a surface film and turbulence with the sum of the decay rates from the surface film and from the turbulence based on the best available knowledge of these processes.

6.1. Theoretical Dispersion Equation for Wave Decay Rate Due to Bulk Viscosity and Surface Film Elasticity

The theoretical decay rate for a film-covered surface comes from the dispersion relation provided in equivalent forms by *Dorrestein* [1951], *Lucassen-Reynders and Lucassen* [1969], *Hansen and Ahmad* [1971] and *Alpers and Huhnerfuss* [1989]. The form given by Hansen and Ahmad is

$$(\rho\omega^2 - Tk^3 - \rho gk)(\rho\omega^2 - mk^2\epsilon) - \epsilon k^3(Tk^3 + \rho gk) + 4i\rho\mu\omega^3 k^2 + 4\mu^2\omega^2 k^3(m-k) = 0 \quad (13)$$

where
ρ density of the water;
ω circular frequency of the waves;
k complex wave number in the longitudinal direction;
g acceleration due to gravity;
ϵ is equal to $E - i\omega\mu_s$ complex surface stiffness;
μ absolute viscosity of the bulk fluid;
μ_s surface viscosity of the surface film;
m complex wavenumber in the vertical direction for the rotational component of the flow, equal to $\sqrt{k^2 - i\omega\rho/\mu}$, where the solution with a positive real part is to be taken.

The complex wavenumber is $k = k_r + ik_i$, where $k_r = 2\pi/\lambda$, and λ is the wave length; k_i is the spatial decay rate of the waves.

Equation (13) has six roots for k for any prescribed value of ω. For transverse waves, which are the subject of the study here, the correct root is the one close to the solution of

$$\omega^2 = gk + \frac{T}{\rho}k^3 \quad (14)$$

The aforementioned references, and others [cf. *Cini et al.*, 1987], give an explicit approximation for the wavenumber in terms of the wave frequency on the basis that it differs little from the solution to (14). However, the approach here is to obtain a more accurate solution for k_r and k_i, by using the solution to (14) as a starting point for applying Newton's method to (13).

M&M showed that the damping rate of transverse waves on a film covered surface is very well explained by the quasi-static film elasticity E and zero surface viscosity for several surface films including those adsorbed from natural seawater surfactants, for the 0 to 25 Hz frequency range of their experiments. Therefore the theoretical basis used here for film-induced wave damping will be based on the static elasticity and zero surface viscosity.

6.2. Empirical Relation for Wave Decay due to Turbulence

O&M developed the following equation for the spatial decay rate, β, of waves due to statistically stationary turbulence:

$$\beta = 0.103 \frac{u_1'}{c_g L_1^{1/3} \lambda^{2/3}} \quad (15)$$

where $c_g \approx d\omega/dk_r$ is the group velocity of the waves and $\lambda \approx 2\pi/k_r$ is the wavelength of the waves.

Application of (15) requires specification of the near surface rms horizontal turbulence velocity u_1' and its integral length scale L_1 at a depth just beneath the near-surface rise in u_1' which occurs with this kind of

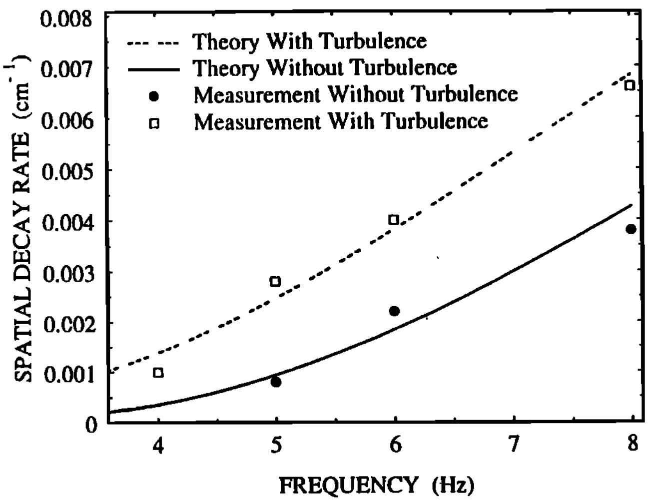

Figure 8. Comparison between the empirical equation for turbulence-induced wave decay and measurements in this study.

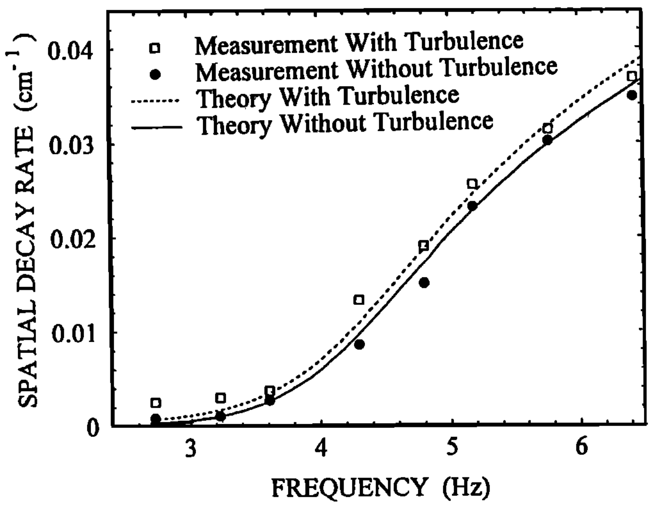

Figure 10. Measured and theoretical spatial decay rates for a Triton X-100 Surface Film.

turbulence. Repeated determination of these quantities by the procedures of section 4 resulted in considerable data scatter between measurements as shown in Figures 6 and 7. From Figures 6 and 7, values of $u_1' = 1.60$ cm/s and $L_1 = 4.25$ cm are used, with the caveat that the prediction of turbulence-induced wave decay is approximate to the extent that $u_1'/L_1^{1/3}$ is approximate.

As described in section 3, since the O&M experiments were done with a different arrangement than was used here, (15) needed to be experimentally confirmed. Figure 8 shows a comparison between (15) and measurements at a few frequencies, analyzed in the way described in section 5. Only a few points were checked since good agreement was found.

7. Results

Figures 9, 10, and 11 show measured and theoretical spatial decay rates for surface films of oleyl alcohol, Triton X-100, and an adsorbed film of natural surfactants on seawater. The data in Figures 9-11 form the principal results of this study.

Theoretical decay rates in the presence of turbulence were taken as sums of the film-induced decay rates k_i and the turbulence induced decay rates β ($\alpha = k_i + \beta$).

The turbulence-induced decay rates are based on values of u_1' and L_1 of 1.65 cm/s and 4.8 cm, respectively, as described in section 6.2. The surface film induced decay rates obtained from the solution to (13) require specification of the surface tension T and the elasticity E. The surface tensions, measured between wave data runs, remained constant to within ±1 mN/m without adjustments required for the Triton X-100 and seawater films.

For the oleyl alcohol film the surface tension was kept constant to within ±1 mN/m, but small amounts of oleyl alcohol needed to be occasionally added to achieve

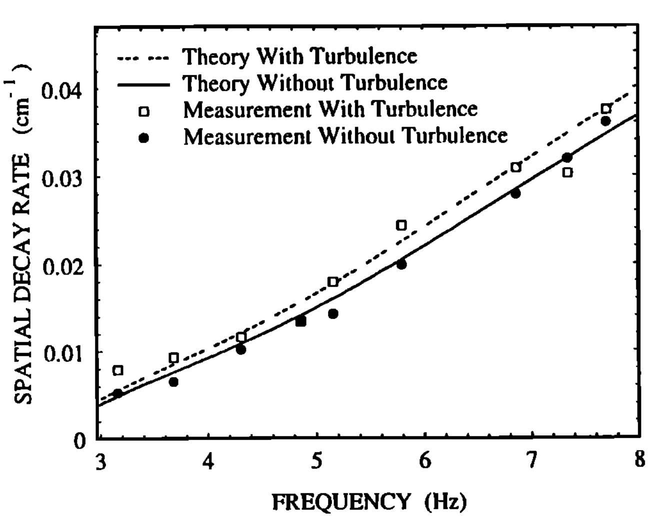

Figure 9. Measured and theoretical spatial decay rates for an oleyl alcohol surface film.

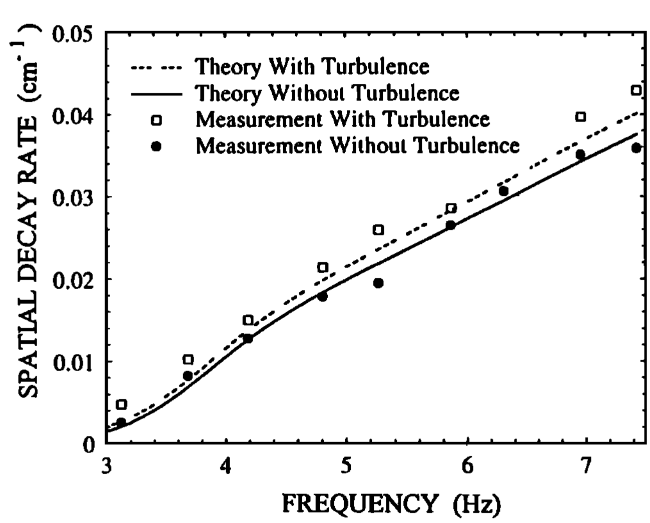

Figure 11. Measured and theoretical spatial decay rates for an adsorbed film of natural surfactants on Seawater.

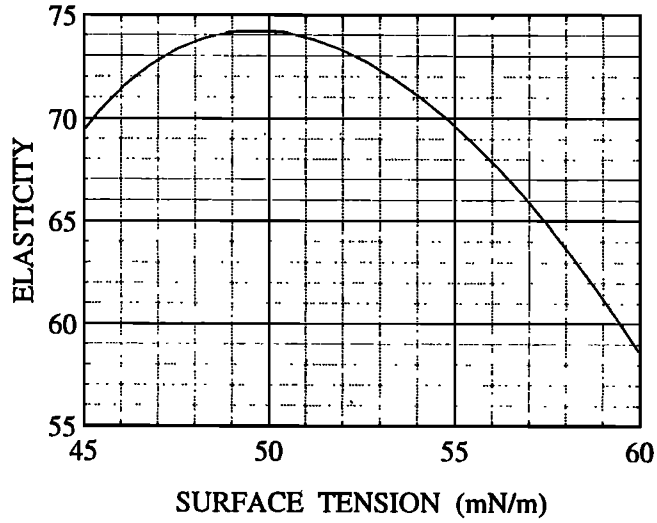

Figure 12. Elasticity versus surface tension for the oleyl alcohol film.

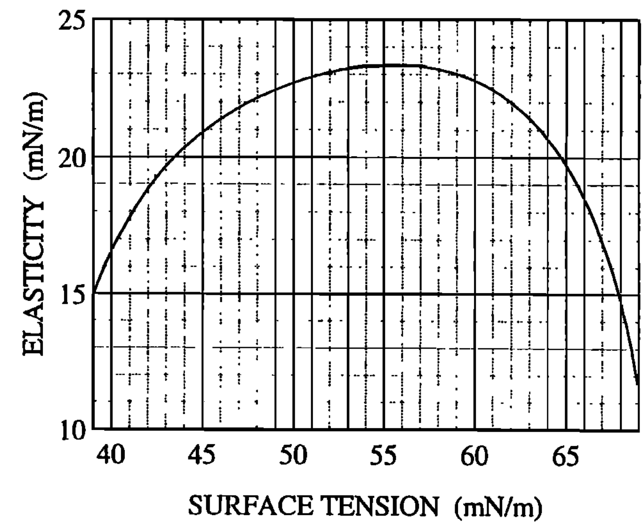

Figure 13. Elasticity versus surface tension for the Triton X-100 film.

this. The total drift in surface tension that would have occurred during the 3.5 hours of testing that would have occurred without the surfactant additions was estimated by adding up the all the changes that occurred each time oleyl alcohol was added. It was found to be 5.2 mN/m which is about 25% of the operating film pressure ($\Pi = T_{\text{clean}} - T$) of 21 mN/m. This is different from that found in the M&M experiments for which the oleyl alcohol film pressure remained constant over long periods of time in a different, and much smaller, tank. The reason why the surface tension increased over time, when oleyl alcohol was not added, occurred in the large tank but did not occur in the small tank is not known with certainty. However, we note that with the large tank it was not possible to nearly eliminate air currents as was done in the small tank, the room temperature was about 8° higher for the large tank experiments which were done in the summer whereas the small tank experiments were not, and it was not possible to use a closed environment with thermal equilibrium with the large tank, but this was achieved with the smaller tank.

Elasticities for the operating surface tensions were determined from the elasticity versus surface tension functions generated from compression isotherms as explained briefly in section 2.2 and in more detail by M&M. Portions of these functions covering the operating surface tensions are shown in Figures 12, 13, and 14.

A slight deviation from the procedure of M&M was necessary for determination of the elasticity versus surface tension for the Triton X-100 film. The other films have timescales for processes that can change the surface tension, other than an area change with its associated immediate surface concentration change, that are long in comparison to the time of a few minutes required to get tension versus area data by repeatedly moving the film barrier, waiting about 15 s, making the measurement for each data point, and moving the barrier to the next position. Triton X-100 has a faster adsorption/desorption or molecular relaxation timescale. It is still long in comparison to wave and turbulence periods but not in comparison to a few minutes. The process for determining the elasticity of the Triton X-100 film was to move the film barrier in continuous motion at a speed of 0.5 cm/s while acquiring surface tension data, on the fly, each time the barrier had moved an additional centimeter. The length of the measurement region went from 65 to 15 cm during the compression. Then the direction of barrier motion was reversed, and data were acquired during the expansion with the length going from 15 to 65 cm. Figure 15 shows the data measured during both the compression and the expansion. When compression is taking place, desorption and/or relaxation processes are taking place and influencing the measured surface tensions. When dilation is oc-

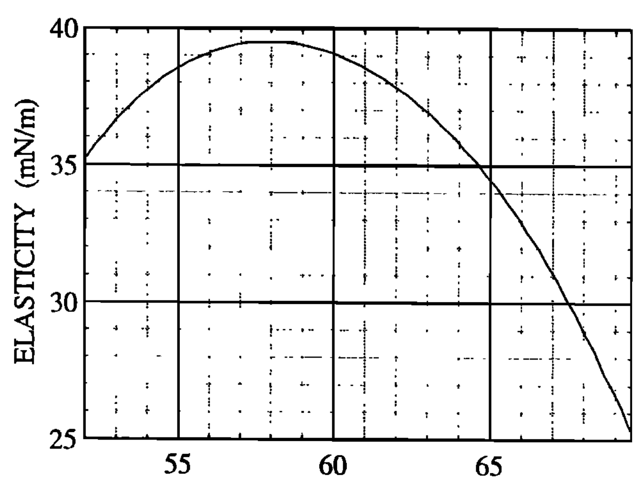

Figure 14. Elasticity versus surface tension for the natural sea surfactant film.

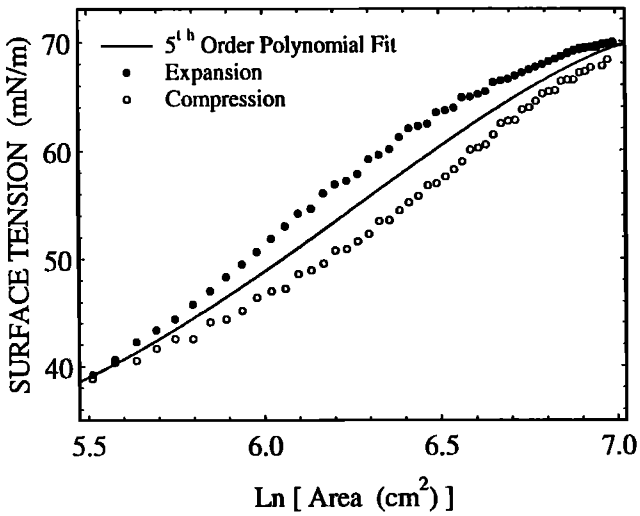

Figure 15. Measured surface tension versus ln (area) for the Triton X-100 surface film during continuous compression and expansion.

curring, these processes influence the measured surface tensions in the opposite way. In order to minimize these influences and achieve the best estimate of the elasticity for comparison of theory with the wave and turbulence experiments, the mean of the two different T versus ln (area) functions (compression and dilation) was then used to represent the desired function since the first-order parts of the time lags cancel each other in the process. For interpolation, a fifth-order polynomial in ln (area) was fit to all the data taken during the compression and the expansion and its derivative is used as the elasticity. The interpolating function is also shown in Figure 15.

Table 1 shows the values of surface tension and elasticity used for obtaining the theoretical surface film induced decay rates.

8. Conclusions

Figures 9, 10, and 11 show that wave decay rates in the simultaneous presence of a surfactant surface film and turbulence are well represented by the sum of the individual surfactant-induced and turbulence-induced decay rates. Although there is considerable "scatter" in the data, particularly when turbulence is present, the average of the deviations between theory and experiment supports this conclusion. The increased data scatter in the presence of turbulence occurs because of limited time duration of the measurements of the randomly varying wave amplitudes.

Thus, for the experiments here, the presence of turbulence did not measurably increase the surface-film-induced wave damping. This finding leads to two further considerations. The first is that the wave-induced oscillating boundary layer probably lies within the viscous sublayer induced by the interaction of the turbulent motion and the free surface, and this sublayer evidently has insufficient mixing to materially increase the surfactant-induced wave damping.

The second consideration is to ask what might happen if the oscillating boundary layer associated with the waves extended below the viscous sublayer of thickness L_v associated with the interaction between the turbulence and the surface. One way to consider this is through the ratio $\mathcal{R}$ of the order of magnitude of the vertical convection distance during half a wave period to the oscillating layer thickness $\sqrt{\nu T}$. O&M analyzed the near-surface turbulence measured by *Brumley and Jirka* [1987], which reached somewhat closer to the surface than the measurements presented in this paper, and found that at depths less than 1.5 horizontal length scales the depth-dependent vertical rms velocity $w'(z)$ was well represented by

$$\frac{w'(z)}{u'_{L_1}} = 0.786 \left[\frac{z}{L_1}\right]^{1/3} \tag{16}$$

where L_1 is taken as its value just beneath its rise near the surface and u'_{L_1} is the horizontal rms turbulence velocity at a depth of L_1. If this estimate is used at the middepth of the thin oscillating layer for the vertical turbulent convection velocity, the ratio $\mathcal{R}$ is given by

$$\mathcal{R} = 0.316 \frac{T^{2/3} u_{L_1}}{L_1^{1/3} \nu^{1/3}} \tag{17}$$

For the wave decay experiments reported here, $\mathcal{R}$ varied from 0.66 to 0.35 over the wave frequency range of 3 to 8 Hz. Although these values are not large enough to say definitively that the turbulence would have increased the surfactant-induced decay rate, it seems probable that this would have been the case. This is an additional indication that the wave-induced oscillating boundary layer was inside the viscous surface layer associated with the turbulence.

With reference to (15), the decay rate of a wave of prescribed length is proportional to the quantity $u'_1/L_1^{1/3}$, which is governed by the turbulence. For the experiments reported here, this ratio was about 1 $\mathrm{cm}^{2/3}/\mathrm{s}$. *Kitaigorodskii et al.* [1983] measured turbulence in the ocean for wind speeds in the range of 5.8 to 11.2 m/s and reported turbulence velocities and dissipation length scales (ℓ). Using the approximate relation, $L_1 = \ell/2$ [cf. *Tennekes and Lumley*, 1972] results in $u'_1/L_1^{1/3} \approx 2\ \mathrm{cm}^{2/3}/\mathrm{s}$ in the ocean measurements. This, by itself would indicate that typical short wave decay rates due to turbulence in the ocean would be roughly double those measured in the laboratory experiments.

Table 1. Surface Tensions and Static Elasticities of the Surfactant Films in the Wave Decay Experiments

Film	T-mN/m	E-mN/m
Oleyl Alcohol	51.6	73.7
Triton X-100	60.0	23.0
Seawater	61.4	38.0

In the light wind conditions under which a surface film can form, the short wave film-induced decay rates are expected to dominate this turbulence-induced decay when a film is present. There are two further considerations regarding the turbulence, however. First, we do not know the ratio $u'_1/L_1^{1/3}$ for the light wind oceanic conditions with certainty. Second, the turbulence structure in the very near surface layer in the ocean is uncertain. For the ocean turbulence data given by *Kitaigorodskii et al.* [1983], $L_v \approx 1$ mm according to (8), and $\mathcal{R}$ is 1.3 for 3 Hz waves and 0.7 for 8 Hz waves. If these values apply to conditions with a surface film on the ocean in lighter wind, they would indicate a greater likelihood of the turbulence increasing the surfactant-induced decay rates in the ocean than in the laboratory experiments. However, another complication is that the laboratory turbulence was generated by a subsurface grid, whereas in the absence of breaking waves, much of the ocean turbulence comes from the wind-induced shear layer at the surface. Although the turbulence structures which influence short waves beneath the viscous layers are probably similar, the detailed turbulence structures in the depth of the thin, wave-induced, oscillating boundary layer may be different.

Acknowledgments. This study was supported by the Fluid Dynamics Program of Office of Naval Research under grant N00014-93-1-0546. The ONR Program Manager was Edwin Rood. His cooperation contributed to the quality of the study.

References

Alpers, W., and H. Huhnerfuss, The damping of ocean waves by surface films: A new look at an old problem, *J. Geophys. Res.*, *94*, 6251–6265, 1989.

Boyev, A. G., The damping of surface waves by intense turbulence, *Isv. Russ. Acad. Sci. Atmos. Ocean Phys.*, *7*, 31–36, 1971, engl. Transl.

Brumley, B., and G. Jirka, Near surface turbulence in a grid–stirred tank, *J. Fluid Mech.*, *183*, 235–263, 1987.

Cini, R., P. Lombardini, and H. Huhnerfuss, Remote sensing of marine slicks utilizing their influence on wave spectra, *Int. J. Remote Sens.*, *4*, 101–110, 1983.

Cini, R., P. Paolo, P. Lombardini, C. Manfredi, and E. Cini, Ripples damping due to monomolecular films, *J. Colloid Interface Sci.*, *119*, 74–80, 1987.

Dorrestein, R., General linearized theory of the effect of surface films on water ripples, *Proc. Amsterdam Acad. Sci.*, *54*, 260–356, 1951.

Green, T., H. Medwin, and J. Paquin, Measurements of surface wave decay due to underwater turbulence, *Nature Phys. Sci.*, *237*, 115–117, 1972.

Hansen, R. S., and J. Ahmad, Waves at interfaces, in *Progress in Surface and Membrane Science*, edited by J. Daniell, M. Rosenburg, and D. Cadenhead, vol. 4, pp. 1–56, Academic, San Diego, Calif., 1971.

Jenkins, G. M., and D. G. Watts, *Spectral Analysis and Its Applications*, Holden-Day, Merrifield, Va., 1968.

Kitaigorodskii, S., and J. Lumley, Wave–turbulence interactions in the upper ocean, I. The energy balance of interacting fields of surface wind waves and wind–induced three–dimensional turbulence, *J. Phys. Oceanogr.*, *13*, 1977–1987, 1983.

Kitaigorodskii, S., M. Donelan, J. Lumley, and E. Teray, Wave-turbulence interactions in the upper ocean, II. Statistical characteristics of wave and turbulent components of the random velocity field in the marine surface layer, *J. Phys. Oceanogr.*, *13*, 1988–1998, 1983.

Lazarev, A., and K. Pokazeyev, Damping effect of surfactants on gravitational-capillary waves, 1, Frequency dependence, *Oceanology*, *26*, 29–32, 1986.

Lucassen-Reynders, E. H., and J. Lucassen, Properties of capillary waves, *Adv. Colloid Interface Sci.*, *2*, 347–395, 1969.

Mass, J. T., and J. H. Milgram, Dynamic behavior of natural sea surfactant films, *J. Geophys. Res, this issue*, 1998.

Milgram, J. H., R. A. Skop, R. D. Peltzer, and O. M. Griffin, Modeling short sea wave distributions in the far wakes of ships, *J. Geophys. Res.*, *98*, 7115–7124, 1993.

Olmez, H., and J. Milgram, Attenuation of water waves by turbulence, *J. Fluid Mech.*, *239*, 133–156, 1992.

Skoda, J. D., The interaction of waves and turbulence in water, Ph.D. thesis, Univ. of Calif., Berkeley, 1972.

Snyder, R. L., F. W. Dobson, J. A. Elliott, and R. B. Long, Array measurements of atmospheric pressure fluctuations above surface gravity waves, *J. Fluid Mech.*, *102*, 1–59, 1981.

Tennekes, H., and J. Lumley, *A First Course in Turbulence*, MIT Press, Cambridge, Mass., 1972.

J. H. Milgram, Department of Ocean Engineering, Room 5-318, Massachusetts Institute of Technology, Cambridge, MA 02139. (email: jmilgram@mit.edu)

(Received September 8, 1997; revised March 4, 1998; accepted April 7, 1998.)